

Synthesis, Crystal Structure, and Spectral Analysis of Antimony Thiourea Tetra Chloride

K. Mahesha Upadhy & N. K. Udayashankar

To cite this article: K. Mahesha Upadhy & N. K. Udayashankar (2010) Synthesis, Crystal Structure, and Spectral Analysis of Antimony Thiourea Tetra Chloride, Synthesis and Reactivity in Inorganic, Metal-Organic, and Nano-Metal Chemistry, 40:10, 812-820, DOI: 10.1080/15533174.2010.522548

To link to this article: <https://doi.org/10.1080/15533174.2010.522548>



Published online: 03 Dec 2010.



Submit your article to this journal [↗](#)



Article views: 160



View related articles [↗](#)



Citing articles: 1 View citing articles [↗](#)

Synthesis, Crystal Structure, and Spectral Analysis of Antimony Thiourea Tetra Chloride

K. Mahesha Upadhya and N. K. Udayashankar

Department of Physics, National Institute of Technology Karnataka, Surathkal, P. O. Srinivasnagar, Karnataka, India

The synthesis of antimony thiourea tetra chloride (ATTC) single crystals by solution technique at room temperature is reported. The complex crystallizes in the orthorhombic space group Pnma with four formula units of $Sb[CS(NH_2)_2]_2Cl_3 \cdot Cl$ in the unit cell. The structure has been solved by direct methods and refined to a final-R value of 0.0393. The synthesized crystals are characterized by FT-IR, UV-visible and TGA-DTA techniques.

Keywords antimony complex, crystal structure, synthesis, thermogravimetric

INTRODUCTION

Single crystals of some inorganic complexes of thiourea are gaining importance in recent years because of their unique optical properties.^[1–3] The thiourea molecule is an interesting inorganic matrix modifier due to its large dipole moment^[4] and its ability to form an extensive network of hydrogen bonds. These metal-organic materials have the potential for combining the chemical flexibility of organics with the physical ruggedness of inorganics. Also, the complexes of some main group elements,^[5] such as antimony, can possess a certain biological function.^[6–8] To synthesize complexes of antimony will be interesting not only for main group element chemistry, but also bioinorganic chemistry.^[9] The present investigation is aimed at the synthesis, structure and spectral analysis of antimony thiourea tetra chloride single crystals.

EXPERIMENTAL

For 100 ml concentrated hydrochloric acid, 9 g of antimony oxide was mixed and the mixture was stirred well and

filtered to get antimony chloride solution. This solution is thoroughly mixed with 9 g of thiourea dissolved in 300 ml of distilled water, filtered and kept at room temperature to get yellow coloured ATTC crystals. As-grown ATTC crystals are shown in Figure 7.

The single crystal XRD data of ATTC have been collected by Bruker SMART using $MoK\alpha$ radiation. The structure was solved by the direct method and refined by the full matrix least-square technique using the SHELXL program. Powder X-ray diffraction studies were carried out using Rigaku X-ray diffractometer with $CuK\alpha$ radiation ($\lambda = 1.540562 \text{ \AA}$) over the range 10° – 50° at a scanning rate of $2^\circ/\text{min}$. The optical absorption spectrum was recorded in the range of 178.75 nm to 876.15 nm using Ocean Optics, Inc. SD2000 fiber optic spectrometer at the room temperature. The FTIR spectrum was recorded in the range of 500 – 4000 cm^{-1} using Nicolet Avatar 330 FT-IR spectrometer by KBr pellet technique. The TG/DTA analysis of dried powder of single crystals of ATTC is carried out in nitrogen atmosphere at a heating rate of 10 K/min using the Thermo-Gravimetric/Differential Thermal Analyzer EXS-TAR6000 TG/DTA 6300.

RESULTS AND DISCUSSION

ATTC crystals were prepared according to the following reaction scheme:



Structural determination shows that the title compound crystallizes in the orthorhombic space group Pnma. The MERCURY 2.2 drawing of the asymmetric unit of this compound is shown in Figure 1. The carbon-sulphur bond distance lies between that of $C=S$ (1.60 \AA) and $C-S$ (1.81 \AA) distances supporting the existence of planar resonance configuration of thiourea.^[2,4] The crystal packing along a-axis is shown in Figure 2. Interactions like $N2 \dots Cl3$, $N1 \dots Cl1$ were found, which can be considered as hydrogen bonds, were responsible for the crystal packing. The crystal data, data collection, refinement details, atomic coordinates, anisotropic atomic displacement

Received 11 July 2010; accepted 26 July 2010.

Address correspondence to K. Mahesha Upadhya, Department of Physics, National Institute of Technology Karnataka, Surathkal, P.O. Srinivasnagar, Karnataka, India 575025. E-mail: mahesh.upadhya@yahoo.com

TABLE 1
Crystal data, data collection, and refinement details

Empirical formula	C ₂ H ₈ Cl ₄ N ₄ S ₂ Sb
Formula weight	415.82
Crystal system, space group	Orthorhombic, Pnma
Cell parameters	a = 13.8015(12) Å α = 90° b = 14.7064(13) Å β = 90° c = 6.0048(5) Å γ = 90°
Number of formula units (Z)	4
Volume	1218.80(18) Å ³
Calculated density	2.266 Mgm ⁻³
Radiation, wavelength	MoKα, λ = 0.71073 Å
θ range for data collection	2.77° to 28.22°
Experimental crystal size	0.26 mm × 0.22 mm × 0.20 mm
Temperature	298 K
Absorption coefficient (μ)	3.447 mm ⁻¹
Absorption corrections (T _{min} , T _{max})	0.424, 0.502 (calculated); 0.468, 0.546 (reported)
*F (000)	796.0
Measured /Independent reflections	12958/1526
Observed reflections	1520 [I > 2σ (I)]
Restraints /No. of parameters refined	4/76
Index ranges	-18 ≤ h ≤ 18, -19 ≤ k ≤ 18, and -7 ≤ l ≤ 7
†R	0.0393 [(F ² > 2σ (F ²))]
w	1/ [σ ² (F _o ²) + (0.0252P) ² + 3.5625P] where P = [(F _o ²) + 2(F _c ²)]/3
Weighted R factor (wR)	0.1142
Goodness-of-fit on F ²	1.208
Measurement	Bruker SMART
Structure drawing	Mercury 1.4.2 using CIF
Refinement	SHELXL97 ¹⁰

*F (000) is the structure factor evaluated in the zeroth-order case h = k = l = 0.

†R (residual disagreement) factor is a measure of agreement between the amplitudes of the structure factors calculated from a crystallographic model and those from the original x-ray diffraction data.

‡w is the weights used in least squares refinement to represent the relative influence an observation should have on the results.

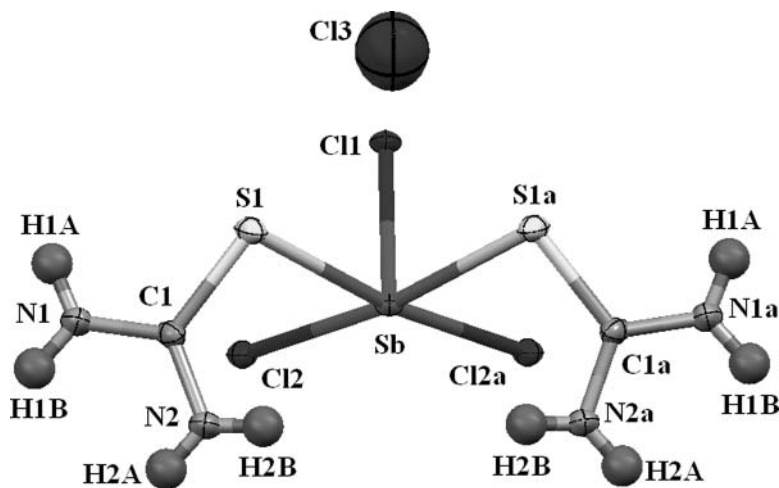


FIG. 1. Asymmetric unit of Sb[CS(NH₂)₂]₂Cl₄. Thermal ellipsoids are shown at 50% probability.

TABLE 2
Atomic coordinates, anisotropic ADPs, and equivalent isotropic ADP for each atom

Atoms	Atomic coordinates			Anisotropic ADPs (\AA^2)						$\dagger U_{\text{equiv}}$ (\AA^2)
	x	y	z	U_{11}	U_{22}	U_{33}	U_{12}	U_{13}	U_{23}	
Sb	0.2874	0.7500	0.0768	0.0150	0.0142	0.0087	0.0000	0.0008	0.0000	0.0126
Cl1	0.2360	0.7500	0.4583	0.0251	0.0178	0.0091	0.0000	0.0029	0.0000	0.0173
Cl2	0.1496	0.6211	0.0170	0.0196	0.0180	0.0136	-0.0031	-0.0012	0.0006	0.0171
Cl3	0.4965	0.7500	0.7614	0.1200	0.0990	0.1120	0.0000	0.0190	0.0000	0.1103
S	0.4087	0.6222	0.2029	0.0221	0.0192	0.0136	0.0048	-0.0045	-0.0028	0.0183
C	0.3851	0.5497	-0.0203	0.0190	0.0164	0.0139	0.0045	-0.0011	-0.0024	0.0164
N1	0.3585	0.4652	0.0197	0.0320	0.0175	0.0145	0.0012	0.0005	-0.0007	0.0213
H1A*	0.352	0.444	0.152	—	—	—	—	—	—	0.0320
H1B*	0.353	0.427	-0.083	—	—	—	—	—	—	0.0320
N2	0.3935	0.5794	-0.2271	0.0330	0.0192	0.0126	-0.0008	0.0003	-0.0010	0.0216
H2A*	0.381	0.544	-0.320	—	—	—	—	—	—	0.0320
H2B*	0.411	0.631	-0.236	—	—	—	—	—	—	0.0320

*Isotropic ADP

$\dagger U_{\text{equiv}}$ is defined as one third of the trace of the orthogonalized U_{ij} tensor whose elements have dimension (length)² and are associated with the mean-square displacements of the atom considered in the corresponding directions.

Symmetry codes: (i) x, y, z (ii) 0.5 -x, -y, 0.5 + z (iii) -x, 0.5 + y, -z (iv) 0.5 +x, 0.5 -y, 0.5 -z (v) -x, -y, -z (vi) 0.5 +x, y, 0.5 -z (vii) x, 0.5 -y, z (viii) 0.5 -x, 0.5 +y, 0.5 +z.

parameters (ADP), and corresponding/equivalent isotropic atomic displacement parameter (U_{equiv}) for each atom, bond lengths, bond angles, torsions and potential hydrogen bonds in the title compound are given in Tables 1-4. The XRD pattern derived from the structural details using crystallographic information file (CIF) is given in Figure 3(a). CCDC 779849 contains the supplementary crystallographic data for this structure. These data can be obtained from The Cambridge Crystallographic Data Centre via www.ccdc.cam.ac.uk/data_request/cif.

The powder X-ray diffraction pattern is shown in Figure 3(b). 2θ and d values of peaks in this XRD pattern are given in Table 5. The indexed hkl values with corresponding 2θ and d values obtained from the structural details using CIF are also listed in Table 5. The d values corresponding to various 2θ values obtained by the powder XRD analysis are in accordance with the d values obtained by the single crystal XRD data. From Figure 3, one can see that each of the experimental diffraction peaks has a corresponding peak

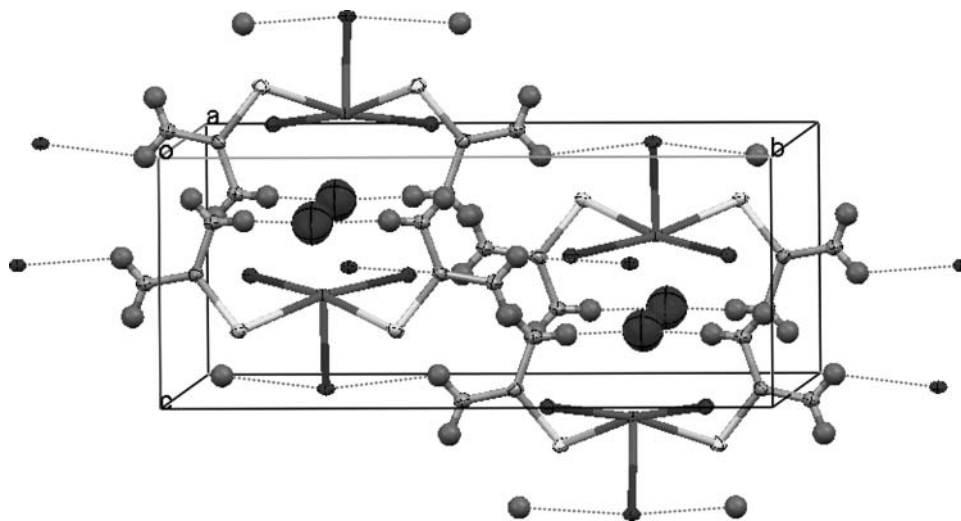


FIG. 2. Projection of the structure of $\text{Sb}[\text{CS}(\text{NH}_2)_2]_2\text{Cl}_4$ along the a axis. The hydrogen bonds are denoted by dotted red lines.

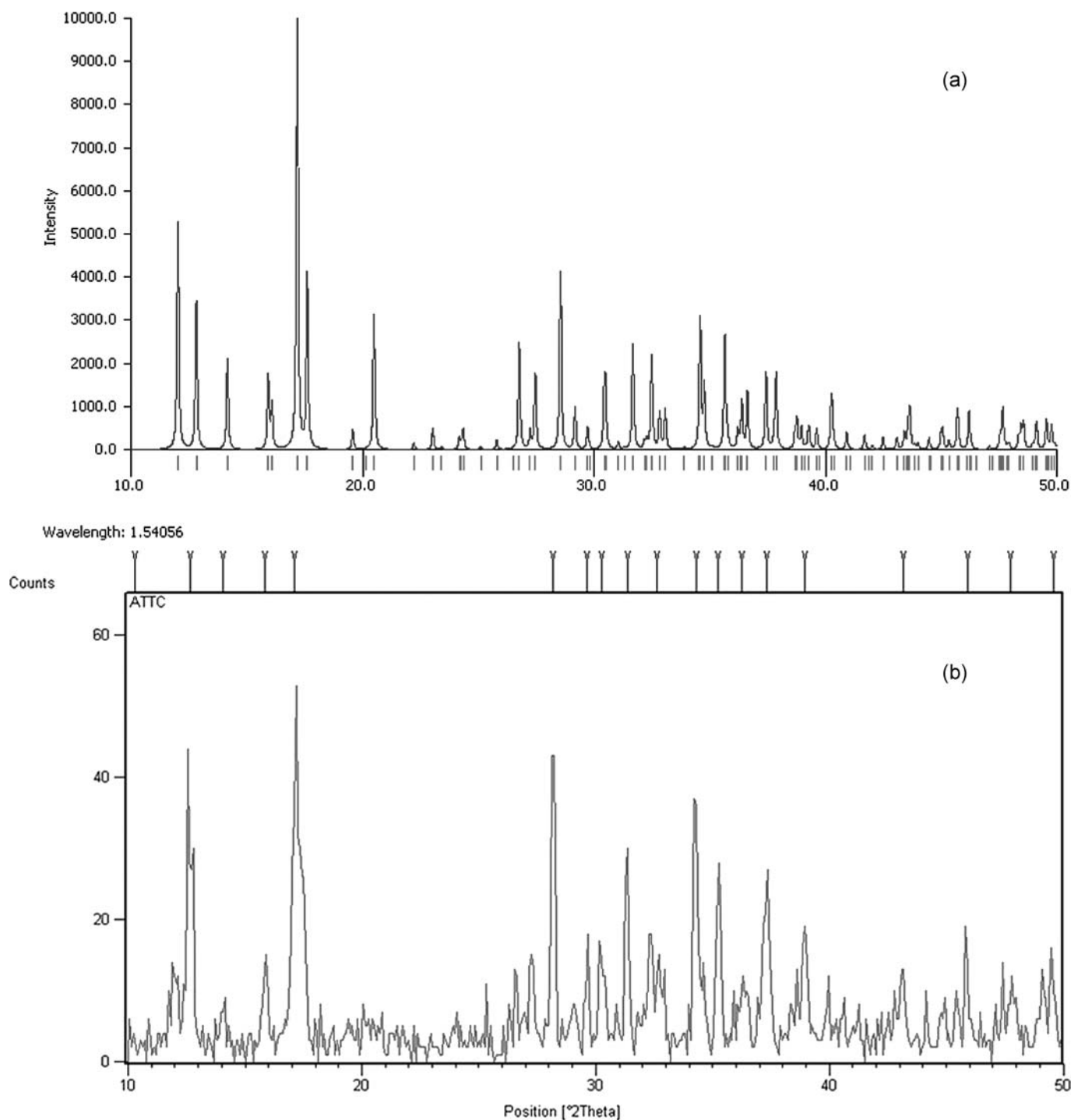


FIG. 3. (a) XRD pattern derived from the structural details using Mercury 2.2; (b) Powder XRD pattern of ATTC.

in the simulated pattern. This indicates that the product is pure.^[11]

UV-Visible Spectra

UV-Visible spectrum of title compound, which was dissolved in 1:1 mixture of N, N-dimethylformamide and tetrahydrofuran, is shown in Figure 4. The absorbance is not reg-

istered due to its excellent optical behavior until the wavelength from 400 nm to 876 nm. Absence of absorption in the region between 400 and 876 nm is an advantage as it is the key requirement for materials having NLO properties.^[12] The visible region of the spectrum exhibits a high intense transition at 298 nm corresponds to the optical band gap of 4.164 eV.

TABLE 3

Bond lengths (Å), bond angles (degree), and torsions (degree) in ATTC

Sb-Cl1	2.398(2) Å	S-C	1.743(5) Å
Sb-Cl2	2.709(1) Å	N1-C	1.318(6) Å
Sb-S	2.628(1) Å	N2-C	1.321(6) Å
N1-H1A	0.86(5) Å	N1-H1B	0.84(6) Å
N2-H2A	0.78(6) Å	N2-H2B	0.80(5) Å
Cl1-Sb-Cl2	85.33(5)°	Cl1-Sb-S	85.03(5)°
Cl2-Sb-S	89.13(4)°	Cl2-Sb-Cl2a	88.81(3)°
Cl2a-Sb-S	170.28(4)°	S-Sb-S	91.31(4)°
Sb-S-C	95.6(2)°	S-C-N1	119.2(3)°
S-C-N2	120.3(3)°	N1-C-N2	120.5(4)°
C-N1-H1A	123(4)°	C-N1-H1B	122(4)°
C-N2-H2A	116(5)°	C-N2-H2B	114(4)°
H1A-N1-H1B	115(6)°	H2A-N2-H2B	131(6)°
Cl1-Sb-S-C	133.9(2)°	Cl2-Sb-S-C	48.5(2)°
Cl2a-Sb-S-C	126.3(3)°	S-Sb-S-C	141.2(2)°
Sb-S-C-N1	-125.3(4)°	Sb-S-C-N2	54.4(4)°
S-C-N1-H1A	0(5)°	S-C-N1-H1B	-173(5)°
N2-C-N1-H1A	-180(5)°	N2-C-N1-H1B	8(5)°
S-C-N2-H2A	-179(5)°	S-C-N2-H2B	1(5)°
N1-C-N2-H2A	1(5)°	N1-C-N2-H2B	-179(5)°

FT-Infrared Spectra

The recorded FTIR spectrum of ATTC is as shown in Figure 5(a). Few peaks were found to be shifted slightly when compared with the spectrum of thiourea^[13,14] due to the following reason. The structure of ATTC reveals that antimony bonds with sulphur as all metals except Ti form complexes via sulphur (Ti forms bond via nitrogen).^[15] Hence the C-S stretching frequency should decrease and that of C-N should increase on complex formation. The absorption at 1618 cm⁻¹ due to NH₂ deformation mode is not affected indicating the absence of nitrogen metal bond. Absorption at 1086 cm⁻¹ due to NH₂ rocking mode is not affected by the formation of metal sulphur bond alone. Thus the metal-sulphur bond is assumed to be responsible for the shifting of the vibration at 1412 cm⁻¹ and 730 cm⁻¹ to a lower frequency.^[15] Comparison of vibrations of thiourea with ATTC crystal is shown in the Table 6.

TABLE 4
Potential hydrogen bonds in ATTC

Donor — H Acceptor	D — H (Å)	H . . . A (Å)	D . . . A (Å)	D — H . . . A (degree)
N2-H2B ..Cl3	0.798	2.111	2.884	163.32
N1-H1B ..Cl1	0.838	2.889	3.443	125.43
N1-H1B ..Cl2	0.838	5.100	5.893	159.88
N1-H1A ..Cl2	0.858	5.749	6.594	169.11

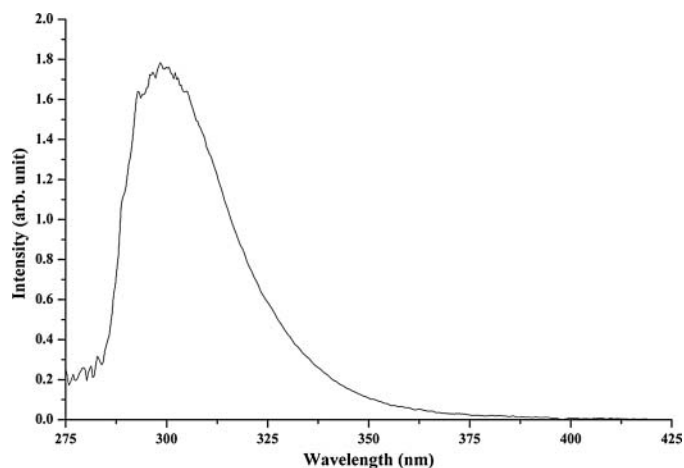


FIG. 4. UV-visible spectrum of the title compound.

Thermogravimetric/Differential Thermal Analysis

Figure 6 shows the TGA and DTA thermogram of ATTC. During the process from 40°C to 189.1°C, it loses weight by the liberation of hydrogen chloride molecules and corresponds to an endothermic peak at 97°C. Here the experimental mass loss (8.77%) is very close to the theoretical one (8.76%) and no phase transformation is observed.

From 189.1°C to 300°C, the weight loss is due to the loss of Cl₂ and CSNHNH₂ (thiocarbazoyl group) from the complex corresponding to an endothermic peak at 247.3°C. At 300°C, the experimental mass loss (42.3%) is close to the theoretical one (43.9%). Now the composition of the product will be Sb[CS(NH₂)₂]Cl. If this composition is reasonable, the theoretical content of Sb in Sb[CS(NH₂)₂]Cl will be 52.2%. A check experiment was conducted by heating the powder of single crystals of ATTC placed in an alumina crucible using muffle furnace. After the furnace temperature rose to 300°C, the sample was kept in the furnace for 10 min. The mass loss (42%) of the sample is close to the theoretical mass loss (43.9%). The atomic absorption spectroscopy using GBC 932 Plus of the heated sample indicates that the relative content of Sb (53.45%) is close to the theoretical content of Sb in Sb[CS(NH₂)₂]Cl. The FTIR spectrum of this decomposition product is shown in Figure 5(b). The absorption at 3326.4 cm⁻¹ is due to N-H band stretching.

From 300°C to 546.9°C, CSNHNH₂ (thiocarbazoyl group), HCl will be eliminated from the complex leading to the endothermic peak at 439.1°C in DTA curve. At 546.9°C, the experimental and theoretical mass losses are 69.1% and 70.7%, respectively. A check experiment was performed by heating the powder of single crystals of ATTC to 547°C and it was kept at that temperature for 02 min. The mass loss (68.1%) of the sample is very close to the theoretical mass loss (70.7%). The atomic absorption spectroscopy of the heated sample indicates that the relative content of Sb in it is 98.1%. This shows that the product at 547°C is metal antimony which

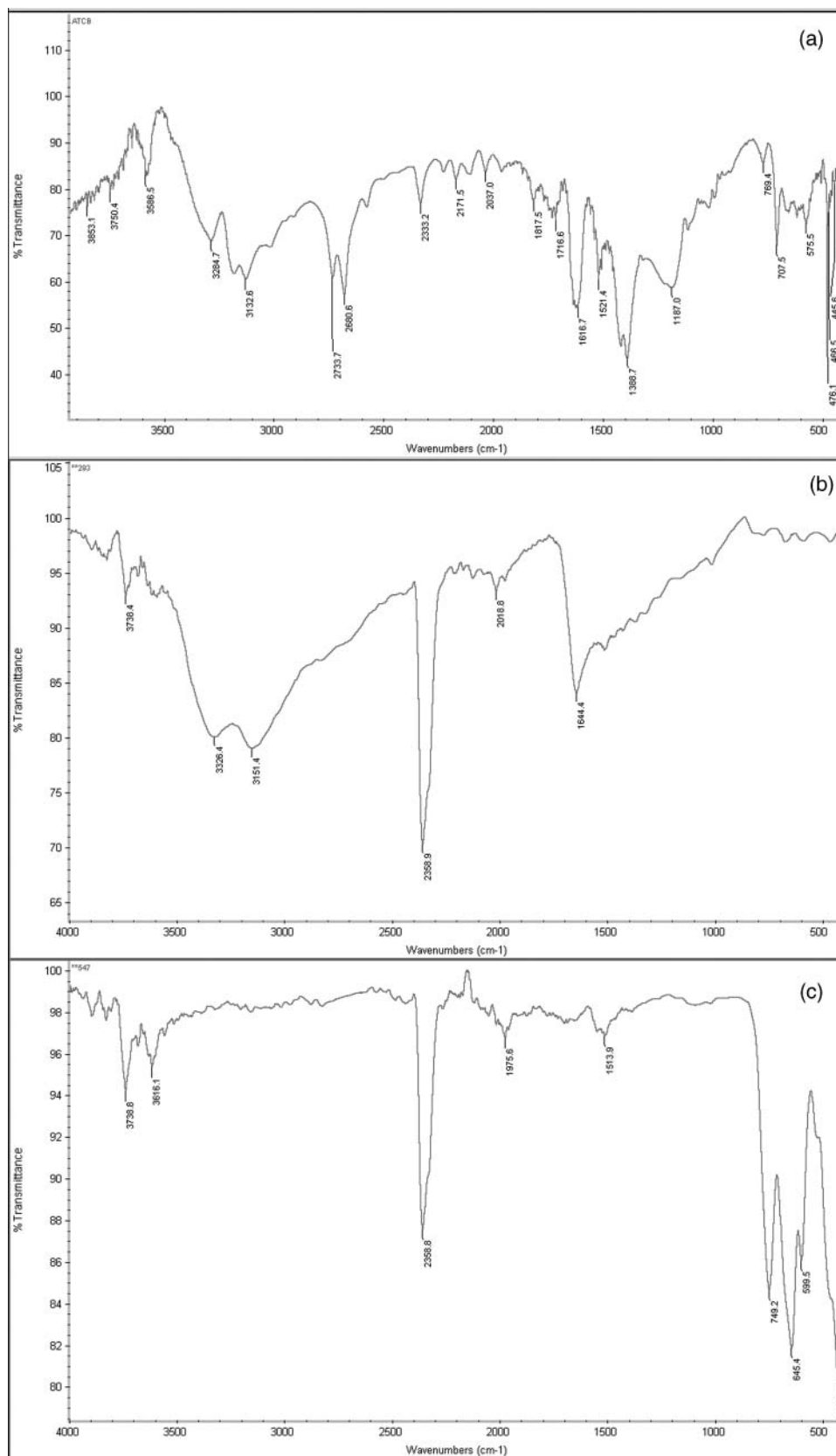


FIG. 5. FTIR spectra of (a) ATTC, (b) decomposition product after heating at 300°C, and (c) decomposition product after heating at 547°C.

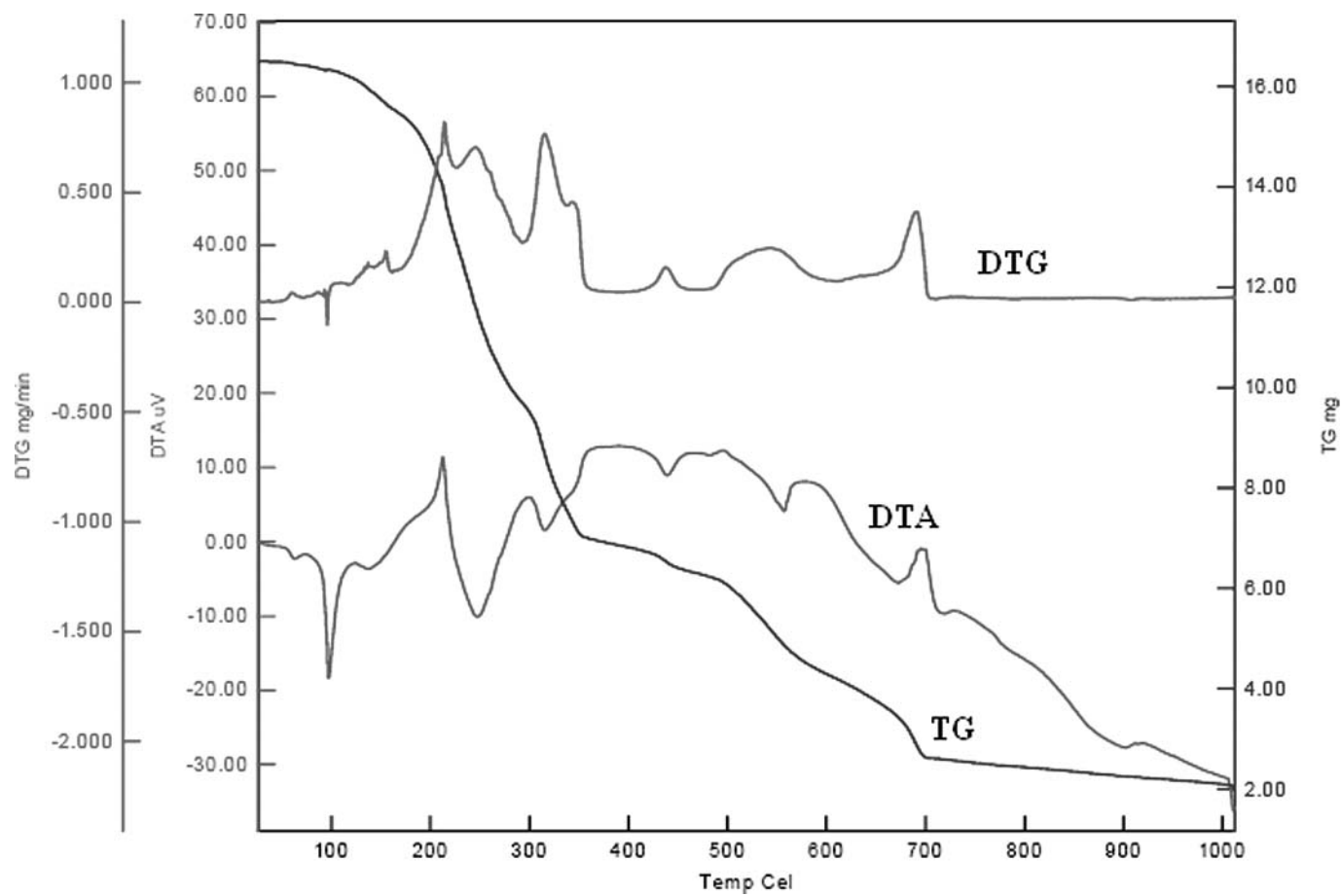


FIG. 6. TGA and DTA thermogram of ATTC.

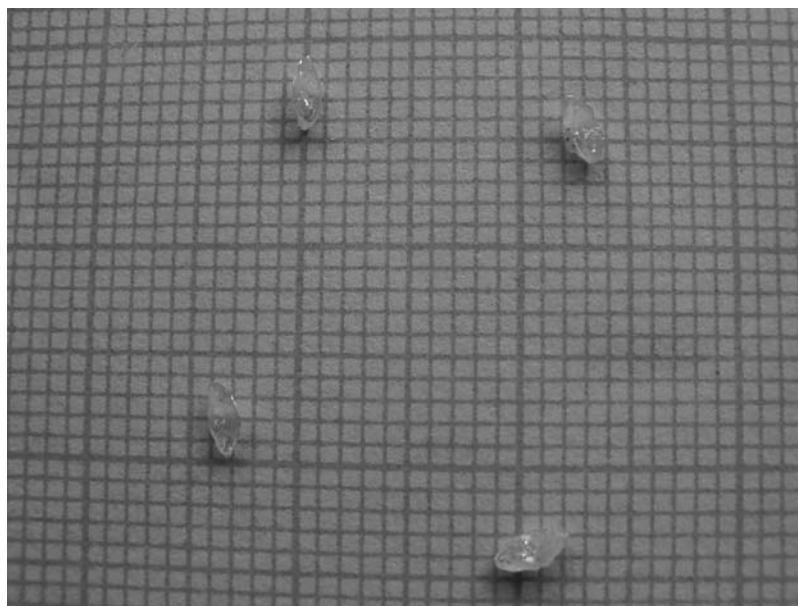


FIG. 7. Photograph of synthesized ATTC single crystals.

TABLE 5
Powder XRD diffraction data for grown ATTC crystals

Data obtained from powder XRD			Data obtained from structural details		
Peak no.	2θ	*d ₁ (Å)	2θ	h k l	d ₂ (Å)
1	10.2688	8.61418	12.043	0 2 0	7.3532
2	12.6614	6.99119	12.826	2 0 0	6.90075
3	14.0604	6.29861	14.196	2 1 0	6.24718
4	15.8499	5.59125	15.957	0 1 1	5.55924
5	17.1253	5.17763	17.196	1 1 1	5.15663
6	28.1813	3.16648	28.543	4 2 0	3.12359
7	29.6249	3.01538	29.717	0 0 2	3.0024
8	30.2714	2.95244	30.500	3 3 1	2.9286
9	31.3494	2.85333	31.283	2 4 1	2.85468
10	32.6007	2.74661	32.522	2 0 2	2.75311
11	34.2877	2.61525	34.543	1 5 1	2.59434
12	35.2497	2.54604	35.130	4 3 1	2.55368
13	36.2540	2.47779	36.239	3 5 0	2.4781
14	37.2973	2.41084	37.804	3 2 2	2.37909
15	38.9650	2.31142	38.978	2 6 0	2.3097
16	43.1385	2.09697	43.413	6 3 0	2.08239
17	45.8989	1.97708	45.761	1 0 3	1.98088
18	47.7607	1.90427	47.652	2 1 3	1.90615
19	49.5624	1.83918	49.543	0 8 0	1.8383

*Here

$$d_2 = \frac{1}{\sqrt{\left[\frac{h^2}{a^2} + \frac{k^2}{b^2} + \frac{l^2}{c^2}\right]}}$$

where a = 13.8015 Å, b = 14.7064 Å, c = 6.0048 Å.

will be volatilized with temperature. The FTIR spectrum of this decomposition product is shown in Figure 5(c). The presence of water modes is due to the absorption of moisture by the product.^[16] The thermal decomposition data is given in Table 7.

TABLE 6

Assignment of IR band frequencies (cm⁻¹) in ATTC crystal

Thiourea	ATTC	Assignment*
3280	3284.7	ν(N-H)
1618	1616.7	δ(NH ₂)
1471	1521.4	ν _{as} (C-N)
1412	1388.7	ν _s (C-S)
1086	1187.0	ρ(NH ₂)
730	707.5	ν _s (C-S)

*δ – Deformation; ν – Band Stretching; ρ – Rocking; s – Symmetric; as – Asymmetric.

TABLE 7
Thermal decomposition data of ATTC crystal

Reaction	DTA (°C)	Mass loss (%)		Sb (%)	
		W _{exp}	W _{theor}	W _{exp}	W _{theor}
Sb[CS(NH ₂) ₂] ₂ Cl ₄					29.282
↓ –HCl	97 (endo)	8.77	8.76		
↓ (40.0°C – 189.1°C)					
↓					
SbC ₂ S ₂ N ₄ H ₇ Cl ₃					32.096
↓ –Cl ₂ , –CSNHNH ₂	247.3(endo)	33.57	35.117		
↓ (189.1°C – 300°C)	300	41.996 ^a			
↓					
Sb[CS(NH ₂) ₂]Cl				53.45 ^b	52.182
↓ –HCl, –CSNHNH ₂	439.1(endo)	26.731	26.833		
↓ (300°C – 546.9°C)	547	68.078 ^a			
↓ Sb				98.11 ^b	100

^aThe percentage mass loss of the sample measured in the check experiment;

^bThe relative content of Sb in the intermediate measured in the check experiment.

CONCLUSIONS

Single crystals of antimony thiourea tetra chloride (ATTTC) were synthesized by solution technique at room temperature. From the single crystal X-ray diffraction pattern, the lattice parameters, molecular structure, molecular weight and volume are found. The presence of functional group of the synthesized complex and the metal-sulphur bond was confirmed by FTIR spectral study. From the absorption spectrum of ATTTC it was found that the ATTTC has good transmittance between 400–876 nm and its optical band gap is also calculated. The TG/DTA analysis revealed no phase transformation of the crystal before and after melting.

REFERENCES

1. Newman, P.R., Warren, L.F., Cunningham, P., Chang, T.Y., Cooper, D.E., Burdge, G.L., PolokDingels, P., and Lowe-Ma, C.K. *Mater. Res. Soc. Symp. Proc.*, **1990**, 173, 557.
2. Venkataramanan, V., Dhanaraj, G., Wadhawan, V.K., Sherwood, J.N., and Bhat, H. L. Crystal growth and defects characterization of zinc tris(thiourea) sulfate: a novel metalorganic nonlinear optical crystal. *J. Cryst. Growth*, **1995**, 154, 92–97.
3. Venkataramanan, V., Bhat, H.L., Srinivasan, M.R., Ayyub, P., and Multani, M.S. Vibrational Spectroscopic Study of the Semiorganic Nonlinear Optical Crystal Bis (thiourea) cadmium chloride. *J. Raman Spectrosc.*, **1997**, 28, 779–784.
4. Hellwege, K.H., and Hellwege, A.M. eds. *Landolt-Börnstein: Numerical Data and Functional Relationships in Science and Technology, Group II*, 14, Springer-Verlag: Berlin, 1982, 584–590.
5. Cantos, G., Barbieri, C.L., Iacomini, M., Gorin, P.A.J., and Travassos, L.R. Synthesis of antimony complexes of yeast mannan and mannan derivatives and their effect on Leishmania-infected macrophages. *Biochem. J.*, **1993**, 289, 155–160.
6. Kaloustian, J., Pauli, A.M., Pieroni, G., and Portugal, H. The use of thermal analysis in determination of some urinary calculi of calcium oxalate. *J. Therm. Anal. Calorim.*, **2002**, 70, 959–973.
7. Xi, L., Yi, L., Jun, W., Huigang, L. and Songsheng, Q. The action of the selenomorpholine compounds on escherichia coli growth by microcalorimetry. *J. Therm. Anal. Calorim.*, **2002**, 67, 589–595.
8. Greenwood, N.N., and Earnshaw, A. *Chemistry of the Elements*, Reed Educational and Professional Publishing Ltd.: Oxford, 1997.
9. Zhong, G.Q., Luan, S.R., Wang, P., Guo, Y.C., Chen, Y.R., and Jia, Y.Q. Synthesis, characterisation and thermal decomposition of thiourea complexes of antimony and bismuth triiodide. *J. Therm. Anal. Calorim.*, **2006**, 86(3), 775–781.
10. Sheldrick, G. M. *SHELXL97, Program for Refinement of Crystal Structures*, University of Gottingen: Germany, 1997.
11. Sun, H.Q., Yuan, D.R., Wang, X.Q., Cheng, X.F., Gong, C.R., Zhou, M., Xu, H.Y., Wei, X.C., Luan, C.N., Pan, D.Y., Li, Z.F., and Shi, X.Z. A novel metal-organic coordination complex crystal: tri-allylthiourea zinc chloride (ATZC). *Cryst. Res. Technol.*, **2005**, 40(9), 882–886.
12. Jagannathan, K., Kalainathan, S., Gnanasekaran, T., Vijayan, N., and Bhagavannarayana, G. Growth and characterization of a novel organic NLO crystal: 4-ethoxy benzaldehyde-n-methyl 4-stilbazolium tosylate. *Cryst. Res. Technol.*, **2007**, 42, 483–487.
13. Shteinberg, B. Ya., Mushkin, Yu. I., and Finkelshtein, A.I. Calculation of the vibrational spectra of urea, thiourea, and their deuterium derivatives. *Opt. Spectrosc.*, **1972**, 33, 589–592.
14. Kemp, W. *Organic Spectroscopy*, second ed., Macmillan: London, 1989, 44–55.
15. Swaminathan, K., and Irving, H.M.N.H. Infra-red absorption spectra of complexes of thiourea. *J. Inorg. Nucl. Chem.*, **1964**, 26, 1291–1294.
16. Kebede, T., Ramana, K.V., and Prasada Rao, M.S. Thermal decomposition of potassium bis-oxalatoaquaindate (III) monohydrate. *Proc. Indian Acad. Sci. (Chem. Sci.)*, **2001**, 113(4), 275–284.